The PML and MTF method based on hybrid finite element method: a comparative study

N. Li[1] , C.H. Zhai[2] and L.L. Xie[2,3]

[1] *PH.D student, School of Civil Engineering, Harbin Institute of Technology, Harbin. China*
[2] *Associate Professor, School of Civil Engineering, Harbin Institute of Technology, Harbin. China*
[3] *Professor, Institute of Engineering Mechanics, Harbin. China*
Email: nealleehit@gmail.com, zch-hit@hit.edu.cn, llxie@iem.net.cn

ABSTRACT :

Perfectly Matched Layer (PML) artificial boundary condition (ABC) gains amount of recognitions because of perfectly performance in the physical wave motion simulations. This paper focuses on the usage of PML method in near-fault earthquake simulations. Combining with velocity-stress hybrid finite element formulation, the applicability of PML is investigated and the numerical reflection of PML is estimated. The reflectivity of PML and multi-transmitting formula (MTF) is compared based on body wave and surface wave simulations. The results show that although PML yields some reflection errors, its absorption performance is superior to MTF boundary in the seismogram simulations, especially in corner and large angle grazing incidence situations. The PML does not arise any unstable phenomenon. The stability of PML is better than MTF boundary in hybrid finite element method. For a specified problem and analysis tolerance, the computational efficiency of PML is only a little lower than MTF.

KEYWORDS: Perfectly Matched Layer, Multi-Transmitting Formula, elastic-dynamic FEM, artificial boundary condition, velocity-stress formulation

1. INTRODUCTION

Nowadays, numerous computational methods have been developed to solve the partial differential equations of physics. The absorbing boundary conditions (ABCs) simulate or replace the infinite space that surrounds a finite computational domain which is used to simulate unbounded domain behavior. However, the replacement is never perfect. The solution computed within an ABC is only an estimate to the solution that would be computed within a really infinite domain. The construction of a suitable ABC is one of the most important problems in unbounded wave propagation simulations. Researchers had proposed many kinds of ABCs, based on kinds of wave motion equations which corresponding to different physical problems. The perfectly matched layer (PML) ABC was firstly proposed by Bérenger (Bérenger, 1994) in his study of electromagnetic wave simulation, which is a non-reflective ABC for any incidence with arbitrary-frequency and arbitrary-incidence angle theoretically.

Researches of PML improved rapidly in the past decay (Bérenger, 2007). The application of PML was extended to 3D Maxwell equation simulations by Chew and Weedon (1994) and Bérenger (1996) at the same time. Chew and Weedon (1994) proposed the concept of PML via a complex-coordinate transform and/or a complementary operators method, which established the theoretical basis for further extending PML to general PDE systems. Thereafter, PML was applied to various PDE systems, such as linearized Euler equation (Hesthaven, 1998), poroelasticity wave equation (Zeng *et al.,* 2001), acoustic equation (Liu and Tao, 1997; Qi and Geers, 1998; Hagstrom and Hariharan, 1998) and elastodynamic equation (Chew and Liu, 1996; Hastings *et al.*, 1996; Collino and Tsogka, 2001; Komatitsch and Tromp, 2003), etc. On the other hand, Collino and Monk (1998) studied the application of PML in curvilinear coordinate system. It should be noted that PML shows some weaknesses in the researches: (1) the applications of PML are limited for the first order PDE systems; (2) it is no longer perfect and yields numerical reflection after numerical discretization (Bérenger, 2007); (3) there is few research contribute PML in seismic wave simulations. In the field of earthquake engineering, Basu and Chopra (2004) studied soil-structure interaction problem with PML, and Zhao *et al.* (2007) applied PML in the simulation of saturated poroelastic wave motion.

Multi-transmitting formula (MTF), which was proposed by Liao and Wong (1984), is another widely used high-precision ABC. Theoretically, MTF boundary is also a non-reflective ABC. However, in the implementation of MTF, it performs instable phenomenon and lower precision than desired. This is partly due to the assumption of incidence as an ideal plane wave motion and some intrinsic factors of numerical algorithm of MTF. In recent years, improvements of precision and stability of MTF was developed (Zhou and Liao, 2001).

PML and MTF boundaries are both high-precision and non-reflective ABCs in theory. However, they both yield reflections after numerical discretization. Because many influencing factors take effect on the reflectivity, it is difficult to define appropriate error criteria for the comparison. This issue is attributed to the different mechanism of the ABCs' numerical reflection yielding. PML adopts specified complementary operators method and modify the constitutive relationship, whereas MTF adopts polynomial approximation and assumption. The adoption of some common phenomenon simulation is the only favorable method to quantities the differences between the ABCs. In addition, a uniform algorithm for inner domain of both ABCs is indispensable since it is essential for obtaining reliable comparative results.

This study presents the theory of PML briefly, especially the 'perfectly matched' characteristic which makes PML can efficiently absorb wave motion with different frequency and incidence angles. Based on the hybrid finite element method, the seismic wave motions are simulated. The applicability of PML in seismic wave simulations is investigated. Based on these preliminary investigations, the reflectivity of PML and MTF ABCs is estimated. Furthermore, the differences between PML and MTF boundary are discussed and the absorption efficiency of these two ABCs is compared.

2. PML and MTF ABCs

1.1 Perfectly matched layer ABC

The basic mathematical principle of PML is introducing a complex coordinate transform into the PDE system. The complex coordinate transform is

$$x_i \to \tilde{x}_i(x) = \int_0^{x_i} s_i(\xi,\omega)\mathrm{d}\xi \quad (1.1)$$

where x_i is the direction of specified coordinate, s_i is some continuous function of variable x_i and ω, respectively. Corresponding to different problems, x_i can takes different form. The function s_i used by Chew and Liu (1996) is defined by

$$s_i = 1 + i\frac{d_i(\xi)}{\omega} \quad (1.2)$$

where $d_i(\xi)$ is the damping function in the direction of x_i and ξ is the distance from PML inner boundary to the integration point, respectively. Based on Eqn. 1.2, it is obviously that $\tilde{x}_i$ in Eqn. 1.1 will be reduced to x_i. The general solution of outlet wave motion is an attenuation wave motion propagating in the PML region. The expression is given by

$$\exp\left[i\omega\left(t - \frac{\boldsymbol{k}}{\omega}\cdot\boldsymbol{x} - \frac{k_i}{\omega}\int d_i(\xi)\mathrm{d}\xi\right)\right] \quad (1.3)$$

Eqn. 1.3 defines wave motion with exponential attenuation ratio. Hereby the energy of wave motion will be absorbed rapidly in PML domain. Due to k_i/ω is the wave speed in the direction of x_i, the attenuation ratio is independent with the wave motion frequency (for non-dispersion wave motion). In the same way, the complex coordinate transform used in Eqn. 1.1 is applied to the partial differential operator, *i.e.* the derivative on x_i direction, the operator will be

$$\frac{\partial}{\partial x_i} \to \frac{\partial}{\partial \tilde{x}_i} = \frac{i\omega}{i\omega + d_i(\xi)}\frac{\partial}{\partial x_i} \quad (1.4)$$

Based on Eqn. 1.1 and 1.4, the wave motion PDE system in PML region can be obtained. The solution of the new wave motion system in PML region maintains the attenuation characteristic in theory.

1.2 Multi-transmitting formula ABC

MTF boundary assumes that the incidence is a plane wave motion. MTF boundary transmits the incident and reflected wave motions to the outside of the boundary using the transmitting concept, and it precedes the transmission several times till the reflection error is small enough. The *N*th order MTF is defined by

$$u_0^{p+1} = \sum_{j=1}^{N}(-1)^{j-1}C_j^N u_j^{p+1-j} \quad (1.5)$$

where $C_j^N = \frac{N!}{(N-j)!j!}$, $u_j^{p+1-j} = u\left((p+1-j)\frac{\Delta x}{c_a}, -j\Delta x\right)$, and c_a is the assumed artificial wave speed, u_0^{p+1} is kinematic variable (velocity, stress or magnetic field intensity, *et al.*) at $(p+1)$ time step on the boundary points, respectively. The most widely used MTF method is the second order MTF, which is given by

$$u(p\Delta t + \Delta t, 0) = 2u(p\Delta t, -c_a\Delta t) - u(p\Delta t - \Delta t, -2c_a\Delta t) \quad (1.6)$$

To gain a better understanding of the development and implementation of MTF boundary, the readers may refer to the book by Liao(2002).

2. Velocity-stress hybrid finite element formulation

The implementation of PML in this study is based on the elasto-dynamic wave motion PDE system. The

Newmark method is adopted to construct PML based on the velocity-stress time staggering scheme. In the numerical algorithm for solving PDE systems, Virieux stagger-grid formulation (Virieux, 1986) is recognized as an efficient method and was widely used in many simulations. This study follows Virieux's stagger-grid concept and adopts hybrid finite element method.
Velocity-stress formula of elasto-dynamic wave motion is defined as (using tensor expression)

$$\begin{cases} \rho\dot{\boldsymbol{v}} = \triangledown \cdot \boldsymbol{\sigma} \\ \boldsymbol{\sigma} = \boldsymbol{c} : \triangledown\boldsymbol{\sigma} \end{cases} \tag{2.1}$$

with the initial conditions, $\boldsymbol{v}(\boldsymbol{x},0) = \boldsymbol{v}_0(\boldsymbol{x})$ and $\boldsymbol{\sigma}(\boldsymbol{x},0) = \boldsymbol{\sigma}_0(\boldsymbol{x})$.
The construction process is based on *Fourior* transform which transforms the time domain wave Eqn. 2.1 into frequency domain wave equation. Substituting Eqn. 1.1 and 1.4 into the frequency domain wave equation, and considering damping function $d_i(\xi)$, then applying the inverse *Fourior* transform, the PML formulation in the boundary region can be obtained (Chew and Liu, 1996). Following the stagger-grid (operator-splitting) concept, the equations are finally given by

$$\begin{matrix} \left(\dfrac{\partial}{\partial t} + d(\xi)\right)\rho\boldsymbol{v}^1 = \triangledown^{\mathrm{V}} \cdot\boldsymbol{\sigma} & \left(\dfrac{\partial}{\partial t} + d(\xi)\right)\boldsymbol{\sigma}^1 = \boldsymbol{c} : \triangledown^{\mathrm{V}}\boldsymbol{v} \\ \dfrac{\partial}{\partial t}\rho\boldsymbol{v}^2 = \triangledown^{\mathrm{P}} \cdot\boldsymbol{\sigma} & \dfrac{\partial}{\partial t}\boldsymbol{\sigma}^2 = \boldsymbol{c} : \triangledown^{\mathrm{P}}\boldsymbol{v} \end{matrix} \tag{2.2}$$

in which, $d(\xi) = \lg\left(\frac{1}{R}\right)\frac{3c_p}{2\delta}\left(\frac{\xi}{\delta}\right)^4$ is the damping function, $\triangledown^{\mathrm{V}} = \boldsymbol{nn}\cdot\triangledown$, $\triangledown^{\mathrm{P}} = (\boldsymbol{I} - \boldsymbol{nn})\cdot\triangledown$ are the splitted gradient operator, where $\boldsymbol{I}$ is the unit matrix, $\boldsymbol{n}$ is the normal direction of absorption boundary, δ is the depth of PML and R is the theoretical reflection ratio, respectively. This operator-splitting operation splits the wave field into two parts. One part is the wave motion propagating in the direction parallel to the boundary, and another is propagating in the direction perpendicular to the boundary. Figure 1 shows the diagram of PML boundary and inner domain.

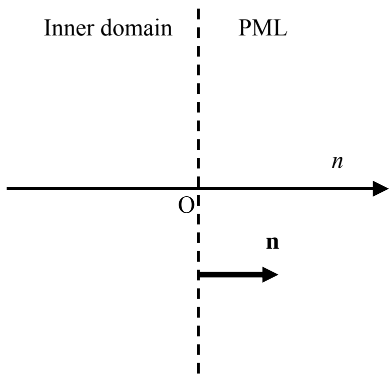

Figure 1 PML problem schedule

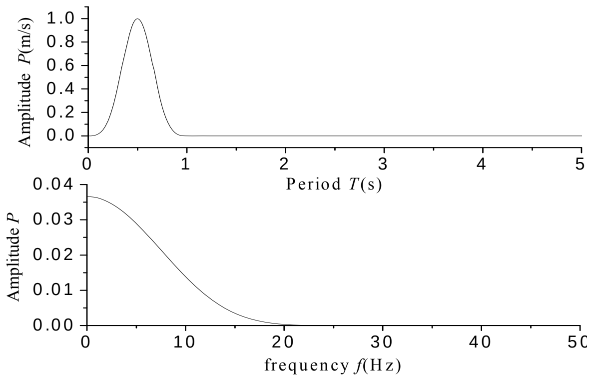

Figure 2 Input excitation information

As a result of varies disadvantages of finite difference-time domain (FDTD) method and finite element method (FEM) algorithm, hybrid method draws more and more attention in recent years (Collino and Tsogka, 2001; Li, *et al.* 2007). In this study, hybrid finite element method was adopted to evaluate the numerical errors.

3. Comparison of PML and MTF

The near-fault seismic wave was simulated using PML and MTF boundaries with pulse-like incidence. The *Ricker* time function was adopted to simulate the incidence, whose time history and frequency component are shown in Figure 2. Figure 4 illustrates model of the body wave simulation. The elasto-dynamic characteristics of the material are as follows: possion ratio v is 0.25, compression wave velocity c_p is 2000m/s and shear wave velocity c_s is 1400m/s. The periphery of the square in Figure 4 uses MTF or PML. Considering the stability requirement, Δt is set as 0.02s. The reflectivity is related to the incidence angle, therefore the responses of corner point (B) and perpendicular incidence points (A and C) are used to illustrate the absorption capacities of the two boundaries. Figure 5 shows the surface wave simulation model. The material properties are the same as body wave simulation. The bilateral vertical sides and bottom boundaries of the square in Figure 5 use MTF or PML boundaries. Different points at different depth from the surface are chosen: point D at the surface, point E at the point under surface 10Δy and point F under surface 40Δy, respectively. The arrows in Figure 4 and 5 demonstrate the loading points and direction of *Ricker* function $p(t)$.

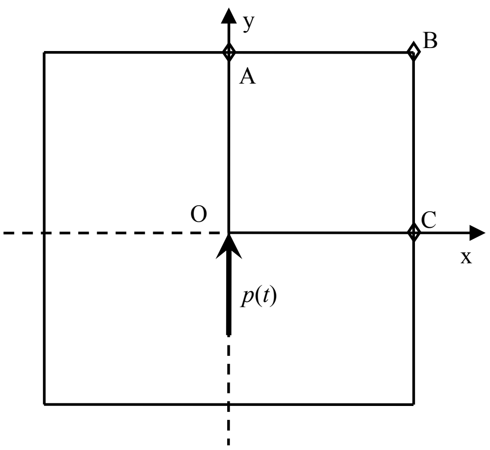

Figure 3 geometry schedule of body wave simulation

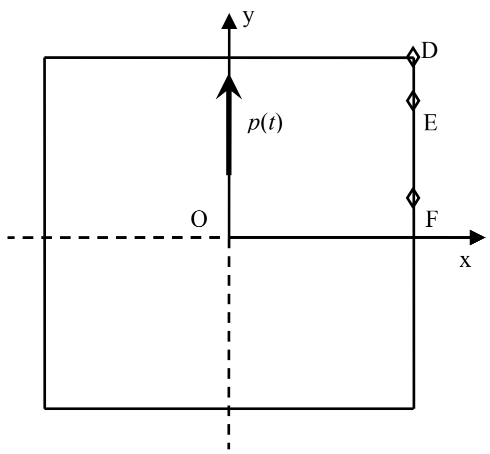

Figure 4 geometry schedule of surface wave simulation

3.1 Comparison based on body wave motion simulation

The velocity response time history at point A, B, and C are computed with two kinds of ABCs. The results are shown in Figure 5(A)-(C), respectively. Some important conclusions can be drawn based on these figures. The absorption capacity of PML is superior to MTF when δ=10, R<10^{-2}. By choosing different parameter R, PML performs a peak reflected value at the same time with different amplitude. *This phenomenon can be rational explained as that the wave motions propagates at the PML outside boundary and yields reflection wave, which travels back into the inner boundary. In order to figure out this phenomenon, the authors carried out amount of numerical examinations.* If the depth of PML increases, the peak reflection value will be lagged. The PML results are almost similar to the analytical result when R<10^{-6}. The PML domain always keeps stable if the inner domain algorithm is stable. Hereby PML possesses better stability performance than MTF.
The absolute value of the errors between numerical and analytical solutions was chosen as the criteria in quantitative comparison. Numerical examinations found that the parameter R plays an important role than δ in these tests. For this reason, the following comparisons keep δ=10 and vary R from 10^{-1} to 10^{-8}. The error values of the comparisons with different parameters are listed in Table 3.1.

Table 3.1 Comparison of finite domain and analytical solution (body wave absorption)

ABCs		*Vx* at A	*Vx* at B	*Vx* at C	*Vy* at A	*Vy* at B	*Vy* at C
MTF		0.0062	0.0079	0.0042	2×10^{-4}	9×10^{-4}	0.0055
PML	R=10^{-1}	0.0161	0.0233	0.0124	0.0019	0.0019	0.0127
	R=10^{-2}	0.0069	0.0104	0.0049	6×10^{-4}	6×10^{-4}	0.0043
	R=10^{-4}	0.0013	0.0021	9×10^{-4}	1×10^{-4}	1×10^{-4}	5×10^{-4}
	R=10^{-6}	3×10^{-4}	5×10^{-4}	2×10^{-4}	$<1\times10^{-4}$	$<1\times10^{-4}$	1×10^{-4}
	R=10^{-8}	1×10^{-4}	1×10^{-4}	1×10^{-4}	$<1\times10^{-4}$	$<1\times10^{-4}$	1×10^{-4}

As illustration in Table 3.1, the numerical error caused by MTF is similar to PML with δ=10, R=10^{-2}. When the incidence is perpendicular to the boundary, the error of MTF is 9% and PML with δ=10, R=10^{-4} is 2%. And when the incidence angle equal to 45 degree, the error of MTF is 6.7% (include geometry damping effect) and PML with δ=10, R=10^{-4} is 1.8%. In the case of R<10^{-6}, the error in the inner domain is less than 0.5%.

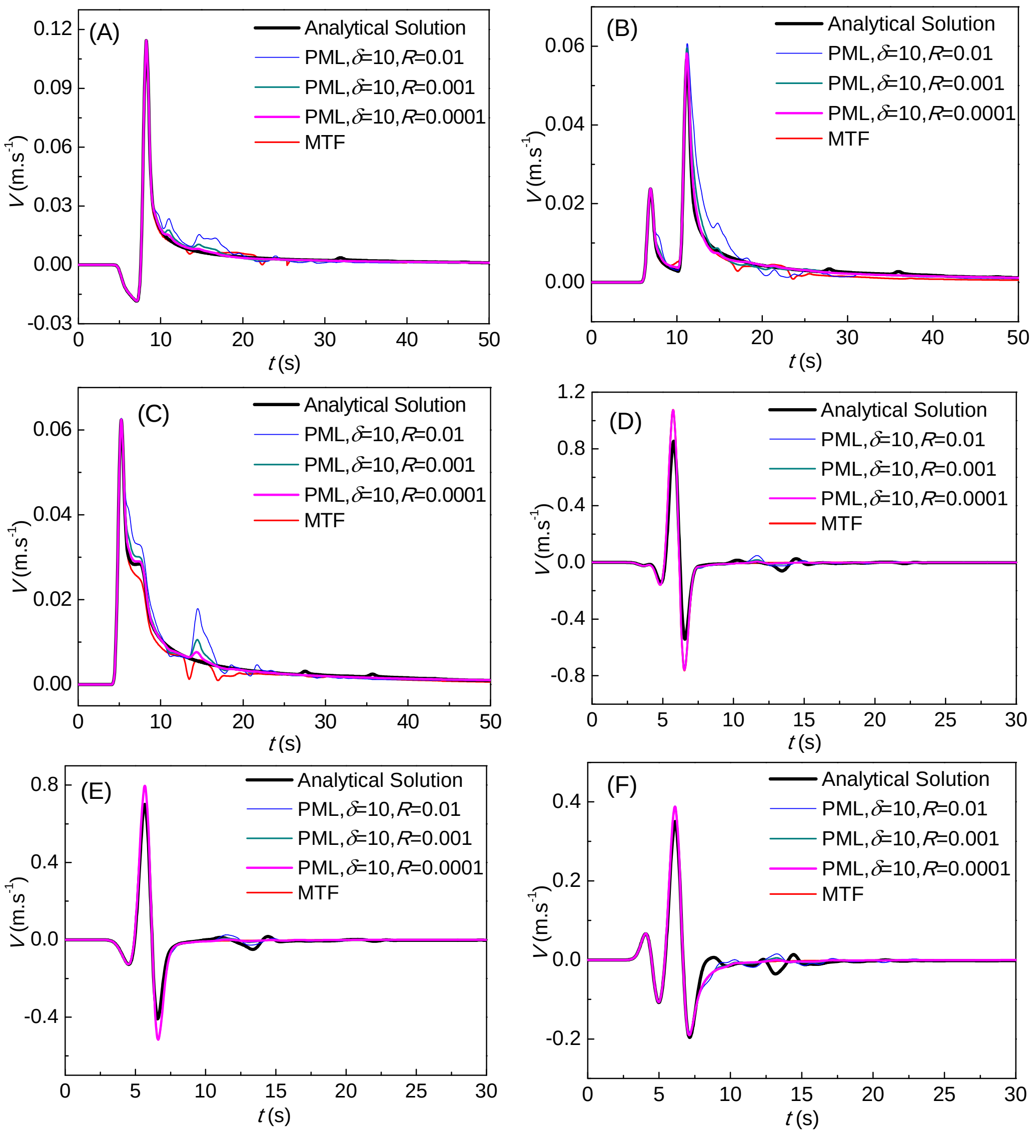

Figure 5 Response time history at points A to F

3.2 Comparison based on surface wave motion simulation

The surface wave simulation model is illustrated in Figure 4. The velocity response time histories at point D, E and F are computed. The results are shown in Figure 5(D)-5(F), respectively. The absorption capacity of PML is better than MTF when δ=10, R<10^{-2}. PML shows a peak reflected value at the same time with different amplitudes as mentioned above. This phenomenon is caused by the incidence wave motion reflected from the PML outside boundary. The PML numerical results are almost similar to the analytical results when R<10^{-6}. The stability of PML is better than MTF.

The absolute value of the errors between numerical and analytical solutions was chosen as the criteria in the quantitative comparison. The comparisons keep δ=10 and vary R from 10^{-1} to 10^{-8}. The errors of the comparisons with different parameters are listed in Table 3.2.

Table 3.2 Comparison of finite domain and analytical solution (surface wave absorption)

ABCs		h=0*	h=1	h=5	h=10	h=20	h=40
MTF		0.0286	**0.0262**	**0.0078**	**0.0104**	0.0085	0.0047
PML	$R=10^{-1}$	0.0231	0.0194	0.0090	0.0183	0.0175	0.0140
	$R=10^{-2}$	0.0096	0.0082	0.0030	0.0045	0.0046	0.0054
	$R=10^{-4}$	0.0018	0.0015	6×10^{-4}	9×10^{-4}	9×10^{-4}	9×10^{-4}
	$R=10^{-6}$	3×10^{-4}	3×10^{-4}	2×10^{-4}	2×10^{-4}	2×10^{-4}	2×10^{-4}
	$R=10^{-8}$	1×10^{-4}	1×10^{-4}	1×10^{-4}	1×10^{-4}	1×10^{-4}	1×10^{-4}

*h is the distance from free surface (unit, Δy)

As shown in Table 3.2, the errors caused by MTF are larger than PML, especially at the near surface boundary points. The errors at surface point (h=0) and the point below surface (h=1) are 4.8% and 4.6%. The numerical errors caused by MTF are larger than PML with δ=10, $R=10^{-1}$, which numerical error is about 3.3%. As the increases the depth h, the reflection error fluctuates within a limit range (boldface number in Table 3.2). When the depth h is about 40Δy, body wave motion dominates the wave motion and the error obtained by MTF is about 6%, which is similar to body wave absorption issue. The absorption capacity of MTF is nearly the same as PML with δ=10, $R=10^{-2}$, which is like the absorption capacity in the body wave simulation.

3.3 The computational efficiency comparison

The computational efficiency of PML is mainly focus on the computation of damping $d(\xi)$. Since the algorithm of PML and inner element is the same, after substituting the function $d(\xi)$ into the stiffness matrix as a material constant, there is no additional computation in PML elements. So there is nearly no increase of computational cost. However, compared with MTF, PML needs to pave several layers of elements (normally 5~20 element length) outside the bounded domain. The computational efficiency of PML will decrease as the layer depth increases and the dimension of the problem increases from 2D to 3D. If the material nonlinearity was considered, the inner domain computations will dominant the efficiency cost. The PML computational cost is very small compared with inner domain cost, because the PML elements will maintain elastic no matter what material the inner domain is. In this study, the computational cost of PML is about 20% more than MTF. The additional costs can be accepted.

Conclusions

In this study, the theory and construction method of PML are presented. The PML is combined with velocity-stress hybrid finite element method, which is then used in the near-fault earthquake simulations. The numerical reflection of PML and MTF boundary are compared. The study leads to the following conclusions.

(1) The numerical reflection of PML is caused by the outside boundary condition; the reflection of MTF is caused by the polynomial interpolation error and the assumption of arbitrary wave speed.

(2) The absorption performance of PML is superior to MTF in the simulations. The absorption capacity of MTF is similar to PML with δ=10, $R=10^{-2}$ for the body wave motion; and the capacity of MTF is similar to PML with δ=10, $R=10^{-1}$ for the surface wave motion.

(3) The absorption capacity of PML can be optimized by tuning the parameter δ and R.

(4) Neither unstable phenomenon nor zero-frequency drift phenomenon has been observed for PML. PML possesses better stability than MTF. The computational cost of PML has not obviously increased.

The comparison procedures in this study also can be used in the estimation of numerical errors, applicability investigation and computation evaluation, and so on. The results in this study are credible for the reason that the comparison procedures are the same and the criteria of numerical errors are unique for the two ABCs. However, some results may be not appropriate for other PDE system; the results should be further investigated.

Acknowledgements

The study was supported by a grant from the National Natural Science Foundation of China (No. 50538050 and No. 90715021). These supports are greatly acknowledged.

REFERENCES

Basu, U., Chopra, A.K. (2004). Perfectly matched layers for transient elastodynamics of unbounded domains. *International Journal for Numerical Methods in Engineering*, **59:8**, 1039-1074.
Bérenger, J.P. (1994). A perfectly matched layer for the absorption of electromagnetic waves. *Journal of. Computational Physics*, **114**, 185-200.
Bérenger, J.P. (1996). Three-dimensional perfectly matched layer for the absorption of electromagnetic waves. *Journal of Computational Physics*, **127**, 363-379.
Bérenger, J.P. (2007). Perfectly Matched Layer for Computational Electromagnetics, Morgan & Claypool, Arizona State University.
Chew, W.C., Weedon, W.H. (1994). A 3-D perfectly matched medium from modified Maxwell's equations with stretched coordinates. *Microwave and Optical Technology Letters.* **13:4**, 599-604.
Chew, W.C., Liu, Q.H. (1996). Perfectly matched layers for elastodynamics: a new absorbing boundary condition. *Journal of Computational Acoustics*, **4:4**, 341-359.
Collino, F., Monk, P. (1998). The perfectly matched layer in curvilinear coordinates. *SIAM Journal on Scientific Computing*, **19:6**, 2061-2090.
Collino, F., Tsogka, C. (2001). Application of the PML absorbing layer model to the linear elastodynamic problem in anisotropic heterogeneous media. *Geophysics*, **66:1**, 294-307.
Hagstrom, T., Hariharan, S.I. (1998). A formulation of asymptotic and exact boundary conditions using local operators. *Applied Numerical Mathematics*, **27**, 403-416.
Hastings, F.D., Schneider, J.B. and Broschat, S.L. (1996). Application of the perfectly matched layer absorbing boundary condition to elastic wave propagation. *Journal of the Acoustical Society of America*, **100:5**, 3061-3069.
Hesthaven, J.S. (1998). On the analysis and construction of perfectly matched layers for the linearized Euler equations. *Journal of Computational Physics*, **142**, 129-147.
Komatitsch, D., Tromp, J. (2003). A perfectly matched layer absorbing boundary condition for the second-order seismic wave equation. *Geophysical Journal International*, **154**, 146-153.
Li, N., Xie, L.L. and Zhai, C.H. (2007). Comparison of perfectly matched layer and multi-transmitting formula artificial boundary condition based on hybrid finite element formulation. *Acta Seismologica Sinica*, **20:6,** 684-695.
Liao, Z.P. (2002). Introduction to Wave Motion Theories for Engineering. Beijing, Science Press.
Liao, Z.P., Wong H.L. (1984). A transmitting boundary for the numerical simulation of elastic wave propagation. *Soil Dynamics and Earthquake Engineering*, **3:4**, 174-183.
Liu, Q.H., Tao, J. (1997). The perfectly matched layer for acoustic waves in absorptive media. *Journal of the Acoustical Society of America*, **102:4**, 2072-2082.
Qi, Q., Geers, T.L. (1998). Evaluation of the perfectly matched layer for computational acoustics. *Journal of Computational Physics*, **139**, 166-183.
Virieux, J. (1986). P-SV wave Propagation in heterogeneous media: Velocity-stress finite difference method. *Geophysics*, **51**, 889-901.
Zeng, Y.Q., He, Q.E. and Liu, Q.H. (2001). The application of the perfectly matched layer in a numerical modeling of wave propagation in poroelastic media. *Geophysics*, **64:6**, 1258-1266
Zhao, H. *et al*. (2007). Applications of the boundary absorption using a perfectly matched layer for elastic wave simulation in poroelastic media. *Chinese Journal of Geophysics,* **50:2**, 581~591.
Zhou Z.H., Liao, Z.P. (2001). A stabilization measure for multi-transmitting formula. *Earthquake Engineering and Engineering Vibration*, **21:1**, 10~14.